Liquid Crystals

Publication details, including instructions for authors and subscription information:
http://www.informaworld.com/smpp/title~content=t713926090

Numerical investigation of surface distortion and order parameter variation in nematics

V. Mocella; C. Ferrero; M. Iovane; R. Barberi

To cite this Article Mocella, V. , Ferrero, C. , Iovane, M. and Barberi, R.(1999) 'Numerical investigation of surface distortion and order parameter variation in nematics', Liquid Crystals, 26: 9, 1345 — 1350
To link to this Article: DOI: 10.1080/026782999204011
URL: http://dx.doi.org/10.1080/026782999204011

LIQUID CRYSTALS, 1999, VOL. 26, NO. 9, 1345–1350

Numerical investigation of surface distortion and order parameter variation in nematics

V. MOCELLA†, C. FERRERO†, M. IOVANE‡ and R. BARBERI‡§*
†European Synchrotron Radiation Facility, B.P. 220, F-38043 Grenoble Cedex, France
‡I.N.F.M.—Istituto Nazionale di Fisica della Materia—Calabria, c/o Dip. Fisica, Università della Calabria, I-87036 Rende (CS), Italy
§Facoltà di Ingegneria, Università di Reggio Calabria, Italy

(*Received 23 October 1998; accepted 17 January 1999*)

We analyse the variations of the director **n** and of the scalar order parameter S of a nematic liquid crystal in contact with a surface which imposes a sinusoidal boundary distortion. The amplitude A of the surface profile and the corresponding wavelength λ vary in ranges compatible with the elastic regime $Aq < 1$, where $q = 2\pi/\lambda$ is the surface wave vector. The analysis is carried out by means of a Landau expansion of the free energy where both **n** and S gradients are taken into account. We obtain an evident coupling between S and **n** in a nematic surface layer of thickness ξ_S of the order of a few hundred Ångstroms. Moreover S can vanish close to the surface if the distortion imposed by the boundary conditions is strong enough. The numerical approach presented in this paper is based on the finite element method.

1. Introduction

The orientation of a liquid crystal (LC) by solid substrates is an invaluable tool for researchers working on mesomorphic materials [1]. The preparation of a LC specimen often requires a knowledge of specific surface treatments to control the interaction between the LC molecules and a solid substrate [2]. Many kinds of LC–solid interactions, such as steric and anisotropic van der Waals forces, are responsible for these macroscopic orientating phenomena that are of both practical and conceptual interest. Several practical methods are known for achieving a controlled LC–alignment on a solid substrate (homeotropic, planar or tilted monostable orientations, as well as multistable easy axes can be obtained), but the competition of the intrinsic LC-ordering and the surface induced effects is a complex problem that is a relevant research subject even for the simplest case of nematic LC (NLC) [3].

Due to the increasing interest in bistable devices based on NLC surface properties, the problem of the influence of the surface morphology on the NLC bulk alignment is, at present, very important. In fact, it has been demonstrated that bistable anchoring conditions for nematics can be obtained both on sub-micrometric anisotropic rough substrates (oblique SiO coating) [4, 5] and by means of periodic micrometric surface structures (bi-gratings made with photosensitive materials [6] or microtextured substrates [7]). Simple elastic models, based on the Berreman approach [8], give unsatisfactory results when strong deformations are present, due to the fact that a local decrease of the nematic order parameter S is expected [9, 10]. This is certainly the case for SiO coated plates [11], but similar effects are expected even close to edges and valleys of micrometric bi-gratings.

Numerical investigations of the effect of the coupling between the order parameter S and the NLC distortion were carried out a few years ago by considering the unidimensional problem of samples with boundary conditions which impose a surface order parameter different from that of the bulk [12, 13]. In ref. [12], two cases of surfaces increasing or decreasing S on the boundary layers were taken into account, showing that, even by considering infinitely strong anchoring conditions on the boundary walls, the spatial variation of S is then equivalent to a finite anchoring energy, which is due to a bulk contribution from the surface layer where $\nabla S \neq 0$. In ref. [13], starting from experimentally measured orientational distributions of NLC molecules on mica substrates, a very low value of S was found and its influence on the nematic distortion in the interfacial region was investigated.

In this paper, we present the results of a numerical study concerning the NLC alignment induced by a sinusoidal boundary surface, in a bi-dimensional case where out-of-plane solutions are not allowed. The present investigation concerns the general case where both

---

*Author for correspondence; e-mail: barberi@fis.unical.it

Journal of Liquid Crystals ISSN 0267-8292 print/ISSN 1366-5855 online ©1999 Taylor & Francis Ltd
http://www.tandf.co.uk/JNLS/lct.htm
http://www.taylorandfrancis.com/JNLS/lct.htm

the distortion and the order parameter variations are considered at the same time in a planar cell of finite thickness in the presence of a distorted nematic texture. It represents an extension of an analytical study published a few years ago [14].

2. The physical problem

The geometry of the problem is shown in figure 1. The boundary surface is assumed to have a sinusoidal profile

$$z = A\sin(qx) \qquad (1)$$

where $q = 2\pi/\lambda$ is the surface wave vector, z is the normal to the average surface $z = 0$ and the NLC is in contact with the upper side of the surface. The amplitude A of the surface profile varies in the range 5–20 Å and its wavelength λ is assumed to be in the range 200–500 Å to ensure that all calculations are carried out in the elastic regime $Aq < 1$ [8, 9]. As in ref. [14], the surface director is assumed to be exactly aligned along the boundary sinusoidal profile (fixed surface distortion) whereas S is completely free at the surface. We note that this assumption is not self-contradictory. In fact from the symmetry point of view, a nematic liquid crystal is characterized by the traceless tensor order parameter $Q_{ij} = S(n_i n_j - 1/3\delta_{ij})$. The scalar order parameter S is given by $S = 3/2\langle (\mathbf{n}\ \ \mathbf{a})^2 - 1/3\rangle$, where **a** is the molecular major axis and the brackets $\langle\ \rangle$ mean a statistical average. In a similar manner, **n** is the statistical average of the molecular direction of the major molecular axis. The physical anisotropies are proportional to S, and the optical axis coincides with **n**. Practically we work on the assumption of a slave-order-parameter surface function. The important point is that from the statistical point of view S and **n** are two independent quantities. Hence, at the surface we can assume **n** fixed and S free.

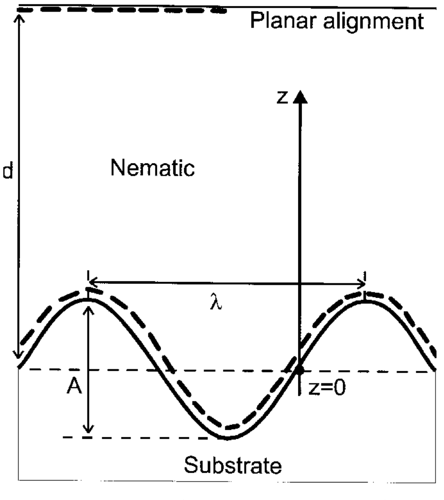

Figure 1. Geometry of the ideal sample. Nematic molecules are assumed to be exactly aligned along the lower boundary sinusoidal profile. A and λ are, respectively, the amplitude and the wavelength of the sinusoidal distortion. The nematic alignment at a distance d from the lower surface is assumed planar.

The model can be generalized by considering a finite surface free energy characterized by an easy axis and an easy surface order parameter. In this manner, the numerical problem is more complicated because the boundary conditions are of the mixed type. This means that they involve the values of the functions and of their derivatives at the surfaces [9], but from the physical point of view the problem remains the same. We limited our analysis to the simpler problem of a fixed surface value of θ [for definition see below] and a free surface value for S, since we focus our attention on the influence on $S(z)$ and $\theta(z)$ of an imposed deformation.

In the bulk, far enough from the geometrical surface, at a distance d much larger than the nematic–isotropic correlation length ξ [1], the alignment is assumed to be planar (parallel to the x-axis): $\theta_{\mathrm{bulk}} = 0$, where θ is the angle between the nematic director **n** and the x-axis associated with the spatial variations of S and θ induced by a surface modulation of the average molecular orientation. It should be noticed that, as we are interested in the coupling of S with variations of **n**, imposing a homeotropic alignment ($\theta_{\mathrm{bulk}} = \pi/2$) or any other uniform alignment, instead, would not have changed the nature of the physical results.

As, in the one elastic constant approximation, there is no direct coupling term between the order parameter variation and the director distortion [10], the NLC volume free energy density can be written as

$$F = g(S) + \frac{3}{4}L_1(\nabla S)^2 + \frac{9}{4}L_1 S^2(\nabla\theta)^2 \qquad (2)$$

where L_1 is the nematic elastic constant. The choice of working in the one elastic constant approximation simplifies the description of the problem, but the lack of direct coupling between the gradients of θ and S does not influence our analysis because we are investigating a sample with a distorted nematic texture. In this case, a spatial change of S always implies a θ variation. The direct coupling between the gradients of θ and S is relevant only when the elastic anisotropy is pronounced, whereas our analysis holds for all nematic materials, even close to the nematic–isotropic transition temperature (as assumed in the following for this problem), where the elastic anisotropy tends to vanish. The direct coupling between the gradient of S and the gradient of θ is an additional source of anchoring and it is expected to change the profile $\theta(z)$, as discussed by Sullivan *et al.* [16, 17]. However, as has been shown recently [18], the direct coupling plays an important role only if the sample is characterized by the same easy axes on the two surfaces. In all the other cases, the initial distortion is the most important source of the subsurface variations of $\theta(z)$ and $S(z)$.

In equation (2), $g(S)$ is the nematic free energy density when S and θ are uniform. It can be expanded in the Landau–de Gennes form in terms of S:

$$g(S) = g(0) + \frac{1}{2}a(T - T^*)S^2 - \frac{1}{3}BS^3 + \frac{1}{4}CS^4 \qquad (3)$$

where $g(0)$ is the free density energy of the isotropic phase of the nematic material; a, B and C are phenomenological parameters independent of the temperature T, and T^* is a temperature close to the nematic–isotropic transition temperature T_C.

The following values, comparable to those available in the literature [7, 19, 20], are assumed for the phenomenological coefficients a, B, C and L_1: $a = 0.065 \times 10^7$ erg cm^{-3} K, $B = C = 2.857 \times 10^6$ erg cm^{-3}, $L_1 = 10^{-6}$ dyn. We fixed $T - T^* = 0.5$ K. With the given values for these physical parameters, one can easily find that, in the bulk far enough from the surface, where S and θ are constant, $F(S)$ has a minimum for $S = S_{\text{bulk}} = 0.65$, which has been assumed as the bulk value of S for our calculations and which is compatible with the experimental values of S for common nematics [1, 20].

The variational statement of the problem, which is based on the principle of minimum energy, was taken as a starting point for the resolution method adopted in this work (see [21] as a general reference). This method has already been described in [22] and will only be briefly recalled here. It consists in finding approximate solutions of the functions $S(x, z)$ and $\theta(x, z)$, minimizing the total free energy $\mathcal{J}(S, \theta)$ of the NLC inside a given region R:

$$\mathcal{J}(S, \theta) = \int_R F(S, \theta)\,\mathrm{d}x\,\mathrm{d}z. \qquad (4)$$

The basic idea of the finite element method (FEM) is to divide the region of interest into small sub-regions (elements) and to approximate the solution functions over each element (piecewise approximation). Following this method, solutions S and θ are sought of the type:

$$S = \sum_{i=1}^{N} N_i(x, z)A_i \quad \text{and} \quad \theta = \sum_{i=1}^{N} N_i(x, z)B_i \qquad (5)$$

where the $N_i(x, z)$ are the so called shape functions, which have to be suitably chosen, and the A_i and B_i are $2N$ unknown coefficients, which can be determined numerically after substituting equations (2), (3) and (5) into (4) and solving the system of equations

$$\begin{aligned} \frac{\partial \mathcal{J}}{\partial A_i} &= 0 \qquad i = 1, 2, \dots, N \\ \frac{\partial \mathcal{J}}{\partial B_i} &= 0 \qquad i = 1, 2, \dots, N \end{aligned} \qquad (6)$$

which are the necessary conditions in order for $\mathcal{J}$ to be at a minimum. A mesh of triangular elements is generated automatically over the integration region R shown in figure 2. A denser element subdivision has been implemented in the neighbourhood of the wall surface, where the larger variations of the functions S and θ are expected. The shape functions are defined locally in every element (triangle) and vanish elsewhere. Under this assumption, the upper limit N of the sums in equation (5) coincides with the number of knots associated to an element. In order to make sure that the values of the functions along the common side of two adjacent triangles match across the border of two elements (C^0 continuity), one can introduce a linear approximation scheme, and particularly the so-called simplex elements [23]. As a consequence, the coefficients (also called 'knot variables') A_i and B_i are assigned the function values in the knot points. The system (6) is non-linear in the variables A_i and B_i and has been solved by means of a non-linear least-square optimization algorithm.

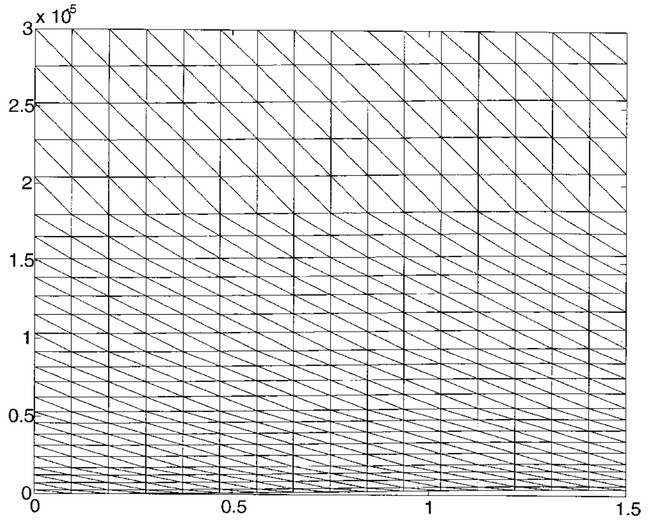

Figure 2. The integration region used in the numerical calculations with the generated mesh of triangular elements. Note the mesh refinement leading to a higher element density in the neighbourhood of the wall surface, where a larger distortion is expected. Units of horizontal and vertical axes are centimeters.

3. Results and discussion

The numerical solutions for $S(z)$ and $\theta(z)$ are actually calculated in the interval $[0, z_{\max} = d]$, with $d = 3 \times 10^3$ Å. Figures 3 to 5 show the variations of the NLC scalar order parameter S and the NLC alignment θ with the distance from the boundary surface, for sinusoidal profiles of amplitude A ranging from 5 to 20 Å. Every plot is drawn for the wavelengths $\lambda = 200$, 300, 400 and 500 Å. In figures 3 (*a*) and 3 (*b*), $S(z)$ and $\theta(z)$ are plotted for $A = 5$ Å. Note that these plots and the following ones for $A = 10$ and 20 Å are traced by considering the variations of $S(z)$ and $\theta(z)$ along a vertical line that crosses the point of maximum slope of the sinusoidal profile of figure 1. This is the region where the nematic distortion is at a maximum and, hence, where the S–θ coupling is expected to be less important. Moreover, we verified that the S–θ coupling is only weakly dependent on the x-coordinate. One may notice that the surface order parameter $S_{\rm surf} = S(0)$ is always lower than that for the bulk, $S_{\rm bulk} = S(d)$. The associated decay length ξ_S is about 2×10^{-6} cm = 200 Å. This can be considered as the thickness of the interfacial region where the nematic properties are different from those of the bulk. As expected, ξ_S is of the same order of magnitude as the coherence length $\xi = [L_1/a(T - T^*)]^{1/2} \approx 125$ Å associated with the nematic order [1]. Figure 3 (*b*) shows that the decay length of $\theta(z)$, ξ_θ, is shorter than ξ_S. This behaviour can be explained by considering that fast variations of θ are favoured by the low nematic order in the interfacial region [13]. Far enough from the lower boundary surface, the distortion of the nematic is practically linear, as expected. The different starting points for the $\theta(z)$ plots are due only to a geometrical effect: as the amplitude A of the surface distortion is fixed and each curve corresponds to a different wavelength λ, the maximum slope $\theta_{\rm surf}$ of a profile depends on λ.

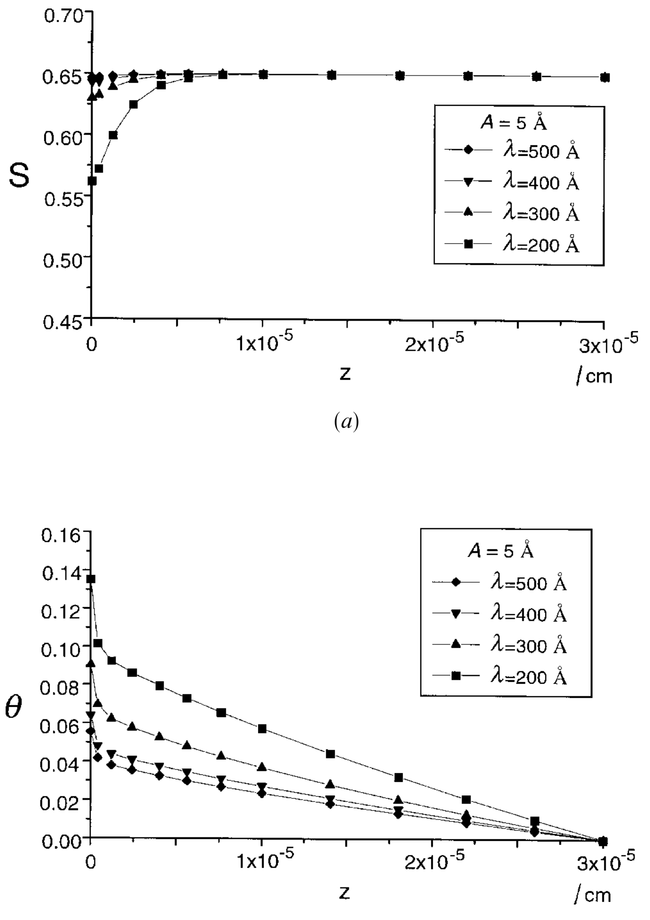

(*a*)

(*b*)

Figure 3. Plots of $S(z)$ (*a*) and $\theta(z)$ (*b*) for sinusoidal surface profiles with amplitude $A = 5$ Å and wavelengths $\lambda = 200$, 300, 400 and 500 Å.

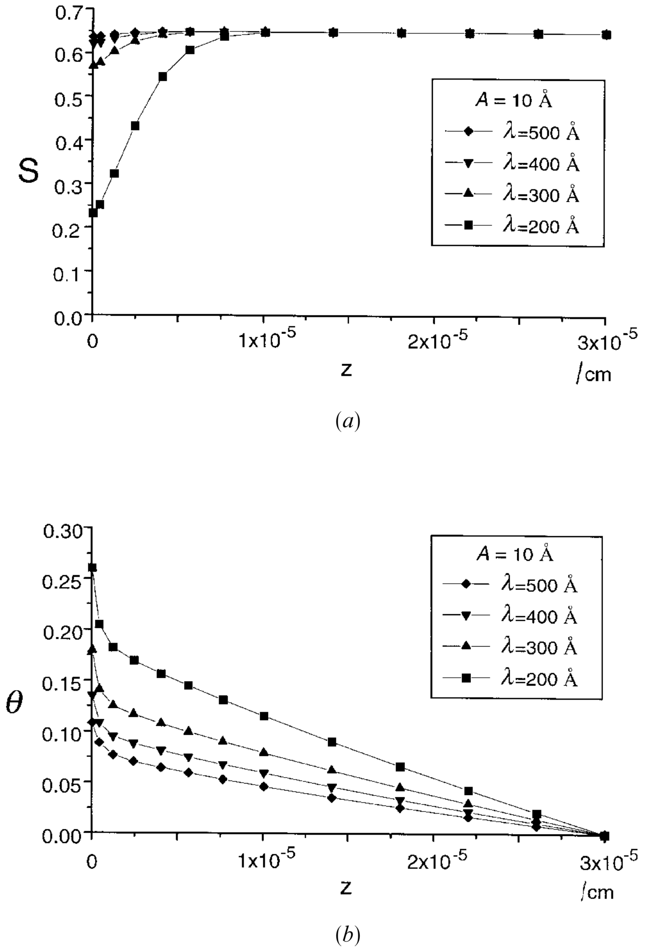

(*a*)

(*b*)

Figure 4. Plots of $S(z)$ (*a*) and $\theta(z)$ (*b*) for sinusoidal surface profiles of amplitude $A = 10$ Å and wavelengths $\lambda = 200$, 300, 400 and 500 Å.

The θ variation along the surface is proportional to A and $1/\lambda$ and, on the other hand, it is coupled to the S variation along the z-direction. This variation occurs over a length which can be one order of magnitude

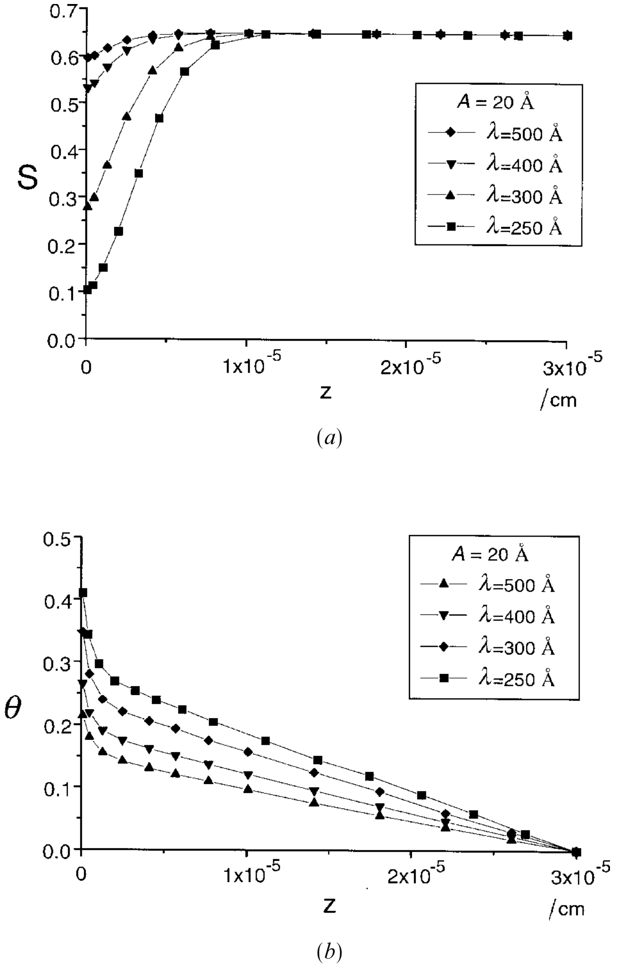

Figure 5. Plots of $S(z)$ (a) and $\theta(z)$ (b) for sinusoidal surface profiles of amplitude $A = 20$ Å and wavelengths $\lambda = 250$, 300, 400 and 500 Å.

larger than the variation along the x-axis. These two competitive effects may give rise to numerical instabilities (like unrealistic oscillations) in the behaviour of θ in extreme cases where large values of A are combined with low λ values, involving dramatic variations of S close to the boundary surface. In our investigations, this turned out to be the case for $A = 20$ Å and $\lambda = 200$ Å. It should be added that the value of S_{surf} is not affected, however, by these instabilities (see figure 6).

Figures 4(a) and 4(b) report the $S(z)$ and $\theta(z)$ curves in the case of $A = 10$ Å. The behaviour is similar to the previous case, but the difference $\Delta S = (S_{\mathrm{bulk}} - S_{\mathrm{surf}})$, for a given λ, is larger. In the case $\lambda = 200$ Å, which corresponds to a stronger nematic surface distortion, S_{surf} reduces to about 0.23, i.e. to a value about three times lower than S_{bulk}.

Plots of $S(z)$ and $\theta(z)$ for $A = 20$ Å are shown in figures 5(a) and 5(b). For $\lambda = 200$ Å, which is not reported here for the reasons described above, S_{surf} practically vanishes. When $\lambda = 250$ Å, we obtain $S_{\mathrm{surf}} \approx 0.1$. It is interesting to note that the starting slope of $S(z)$, $\mathrm{d}S/\mathrm{d}z|_{z=0}$ is lower than the maximum one, enlarging the size of the interfacial region.

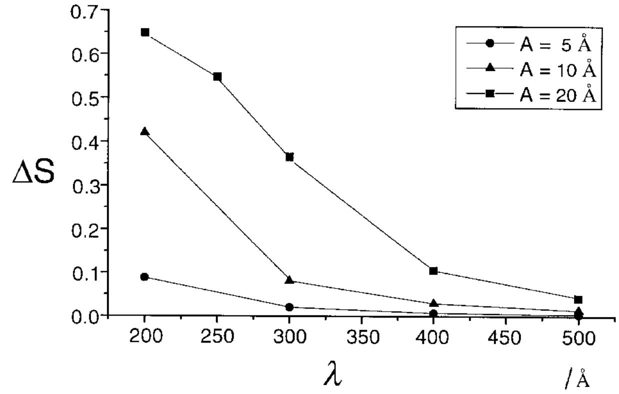

Figure 6. Plots of $\Delta S = (S_{\mathrm{bulk}} - S_{\mathrm{surf}})$ vs. the wavelength λ of the sinusoidal surface profiles for the three cases $A = 5$, 10 and 20 Å.

Figure 6 reports $\Delta S(\lambda)$ for the three cases considered, $A = 5$, 10 and 20 Å. It is evident that even quite a small boundary distortion (such as that usually considered in the limit of a pure elastic description) as in the case $A = 20$ Å, $\lambda = 400$ Å, induces a meaningful variation of S_{surf} with respect to S_{bulk}. A direct consequence is that further effects due to local nematic order variation [24] should then be included in the description of the nematic state close to the boundary surface.

4. Conclusion

Although it has been known for a quite long time that the coupling between the spatial variation of S and θ influences the interfacial layer of a nematic liquid crystal, inducing deviations from the bulk linear distortion in the absence of any external field, these effects were considered to be relevant only in presence of very strong distortions (such as close to a defect or to very rough substrates [11]). Our results provide evidence that large order parameter gradients are also expected close to relatively smooth substrates, reducing the range of application of pure elastic models where S variations are not taken into account.

This result is not completely obvious because S is defined by means of an average over small but macroscopic volumes of nematic. A rough surface, characterized by a strong local anchoring, increases the dispersion of the molecular orientations onto the surface itself, and hence reduces the surface order. Nevertheless, this effect is related to the size of the volume where the averaging process is carried out, but in our analysis this size does not appear explicitly. In fact, it is implicitly defined by the coefficient of the Landau–de Gennes development we used. We recall that this description is suitable only in the case of short range interactions. Then, the order reduction in the layer ξ_S is due to the fact that molecules close to the surface are in contact with the 'disordered' molecular arrangement given by the surface itself.

Many thanks are due to G. Barbero for useful discussions on the physics of the problem and for a critical reading of the paper. This research is partially supported by the European Thematic Network, BriteEuRam programme, Contract No. BET2-0503-96 and by the INFM-Progetto Sud.

References

[1] De Gennes, P. G., and Prost, J., 1993, *The Physics of Liquid Crystals* (Oxford: Clarendon Press).

[2] Cognard, J., 1982, *Mol. Cryst. liq. Cryst. Suppl.*, **1**, 1.

[3] Jérôme, B., 1991, *Rep. Prog. Phys.*, **54**, 391.

[4] Monkade, M., Boix, M., and Durand, G., 1988, *Europhys. Lett.*, **5**, 697.

[5] Jérôme, B., Pieranski, P., and Boix, M., 1988, *Europhys. Lett.*, **5**, 693.

[6] Brown, C. V., Bryan-Brown, G. P., and Hui, V. C., 1997, *Mol. Cryst. liq. Cryst.*, **301**, 163.

[7] Qian, T. Z., and Sheng, P., 1996, *Phys. Rev. Lett.*, **77**, 4564.

[8] Berreman, D. W., 1972, *Phys. Rev. Lett.*, **28**, 1683.

[9] Barbero, G., and Durand, G., 1991, *J. appl. Phys.*, **69**, 6968.

[10] Barbero, G., and Durand, G., 1991, *Mol. Cryst. liq. Cryst.*, **203**, 33.

[11] Papanek, J., and Martinot-Lagarde, Ph., 1996, *J. Phys. II Fr.*, **6**, 205.

[12] Barberi, R., Giocondo, M., Sayko, G. V., and Zvezdin, A. K., 1994, *J. Phys. Condens. Matter*, **6**, A275.

[13] Barberi, R., Barbero, G., and Ferrero, C., 1993, *Mol. Mat.*, **3**, 77.

[14] Jérôme, B., 1994, *J. Phys. Condens. Matter*, **6**, A269.

[15] Barbero, G., and Durand, G., 1991, *J. Phys. II*, **1**, 651.

[16] Sen, A. K., and Sullivan, D. E., 1987, *Phys. Rev. A*, **35**, 1391.

[17] Texeira, P. I. C., Sluckin, T. J., and Sullivan, D. E., 1993, *Liq. Cryst.*, **14**, 1243.

[18] Skacej, G., Alexe-Ionescu, A. L., Barbero, G., and Zumer, S., 1998, *Phys. Rev. E*, **57**, 1780.

[19] Priestley, E. B., Wojtowicz, P. J., and Sheng, P., 1974, *Introduction to Liquid Crystals* (New York: Plenum Press).

[20] Vertogen, G., and de Jeu, W. H., 1988, *Thermotropic Liquid Crystals, Fundamentals* (Berlin, Heidelberg: Springer-Verlag).

[21] Mikhlin, S. G., 1988, *Variational Methods in Mathematical Physics* (New York: Pergamon Press).

[22] Ferrero, C., Mocella, V., Sánchez del Río, M., and Barberi, R., 1997, *Mol. Mat.*, **9**, 109.

[23] Rao, S. S., 1988, *The Finite Element Method in Engineering* (New York: Pergamon Press), pp. 129–131.

[24] Barbero, G., Dozov, L., Palierne, J. F., Durand, G., 1986, *Phys. Rev. Lett.*, **56**, 2056.